Proceedings of Engineering & Technology (PET)
pp. 114-118

Control of the Methane Flame Behavior by the Hydrogen Fuel Addition: Application to Power Plant Combustion Chamber

Fethi BOUARS[1,2] and Mohamed El Hadi ATTIA [1]
[1]Department of physics,University of HL-El Oued,
El Oued, Algeria

Email: f.bouras@hotmail.fr

Fouad KHALDI[2] and Mohamed SI-AMEUR[3]
[2] LPEA Laboratory, Department of Physics
University of HL-Batna,
Batna, Algeria
[3] LESEI Laboratory, Department of Mechanics
University of HL-Batna,
Batna, Algeria

***Abstract*—The present study illustrates a numerical investigation of the turbulent combustion in a burner of power plant supplied by Methane and/or Hydrogen. The computations are carried out by FLUENT-CFD, where the obtained results are validated with experimental reference data. Therefore, the same configuration is used to control the behavior of the velocity field, the temperature field and the mass fraction of carbon monoxide for different percentages of the hydrogen fuel injection in the combustion chamber. Results show that the hydrogen fuel addition has an impact on all physical and chemical parameters of the reactive system.**

***Keywords*— *Turbulent Combustion; Hydrogen/ Methane Flame; Power plant burner; Computational Fluid Computational* .**

I. INTRODUCTION

Recent studies demonstrated the benefits of using hydrogen as a support fuel in hydrocarbon fuel burners. This technique could be a promising solution for the enhancement of combustion processes and to overcome in particular some environmental issues [1]. Some works showed that the enrichment of combustion process by H_2 has effects on reactions zone location, on concentration of OH radicals, on peak temperature and in consequence on NOx emissions [2].
Studying the H_2 fuel addition in a non-premixed turbulent combustion burning in a cylindrical burner is an appropriate configuration of many academic and industry reasons. This configuration is representative of combustion systems in gas turbine power plants. And it was the subject of intensive research activities, experimental as well as numerical [3,4]. With the development of CFD tools and rapidly expanding computer capacity, turbulent models emerge as a tool for simulating 3D combustion that occurs in relatively complex systems [3-5]. Among studies interested in the interaction of turbulence/ chemistry for the non- premixed combustion, we have cited Bouras *et al.* where focusing on a scalar dissipation rate fluctuations in non-premixed turbulent combustion using a stochastic approach [3,4].
In the present work, the behaviors of aerothermochemical parameters are studied in the cylindrical burner fueled by CH_4 and/or H_2. The computations modeling are carried out using the LES model coupled with PDF approach to surmount the closure in the turbulent terms in the governing equations. The effect of the hydrogen enrichments on the velocity, temperature and carbon monoxide is tested for different compositions of the fuel. Results show that the hydrogen addition has an impact on the flame behavior.

II. GOVERNING EQUATIONS

The turbulent combustion can be written in Cartesian coordinates as [3-9]:

Continuity:
$$\frac{\partial \bar{\rho}}{\partial t}+\frac{\partial}{\partial x_i}(\bar{\rho}\tilde{u}_i)=0 \quad (1)$$

Momentum:
$$\frac{\partial \bar{\rho}\tilde{u}_i}{\partial t}+\frac{\partial}{\partial x_i}(\bar{\rho}\tilde{u}_i\tilde{u}_j)=-\frac{\partial}{\partial x_i}[\bar{\rho}(\overline{u_iu_j}-\tilde{u}_i\tilde{u}_j)]-\frac{\partial \bar{p}}{\partial x_j}+\frac{\partial \overline{\tau_{ij}}}{\partial x_i} \quad (2)$$

Energy:
$$\frac{\partial}{\partial t}\overline{\rho}\tilde{h}+\frac{\partial}{\partial x_i}(\bar{\rho}\tilde{u}_i\tilde{h})=-\frac{\partial}{\partial x_i}[\bar{\rho}(\overline{u_ih}-\tilde{u}_i\tilde{h})]+\frac{\partial \bar{p}}{\partial t}+\frac{\partial}{\partial x_i}\overline{u_j\tau_{ij}} \quad (3)$$

Species:
$$\frac{\partial}{\partial t}\overline{\rho}\tilde{Y}_f+\frac{\partial}{\partial x_i}(\bar{\rho}u_i\tilde{Y}_f)=-\frac{\partial}{\partial x_i}[\bar{\rho}(\overline{u_iY_f}-\tilde{u}_i\tilde{Y}_f)]+\bar{\omega}_f \quad (4)$$

Where: $i=1, 2, 3$ and $j=1, 2, 3$

Thermodynamic state:
$$\bar{p}=\bar{\rho}R_m\tilde{T} \quad (5)$$

- Unresolved Reynolds stresses $(\overline{u_iu_j}-\tilde{u}_i\tilde{u}_j)$, requiring a subgrid scale turbulence model.
- Unresolved species fluxes $(\overline{u_iY_f}-\tilde{u}_i\tilde{Y}_f)$ and enthalpy fluxes $(\overline{u_ih}-\tilde{u}_i\tilde{h})$ requiring a probability density function (PDF) approach.
- Filtered chemical reaction rate $\bar{\omega}_f$.

ISSN: 2356-5608

III. Dynamic Turbulence Modelling

A. Large Eddy Simulation Model

The tensor of the unsolved constraints τ_{ij} as the tensor velocity of deformation $\tilde{S}_{ij}$ for subgrid models by the intermediary of a turbulent viscosity (ν_t), and a subgrid kinetic energy (k_{ll}). Therefore, we focus on the assumption of Boussinesq in which the small scales influence the large scales via the subgrid-scale stress [3-9]:

$$\tau_{ij} = 2\overline{\rho}\nu_t \tilde{S}_{ij} - \frac{1}{3}k_{ll}\delta_{ij} \quad (6)$$

Where, the filtered strain rate tensor is defined by:

$$\tilde{S}_{ij} = \frac{1}{2}\left(\frac{\partial \tilde{u}_i}{\partial x_j} + \frac{\partial \tilde{u}_j}{\partial x_i}\right) - \frac{1}{3}\tilde{u}_{ll}\delta_{ij} \quad (7)$$

The candidature of this WALE-eddy viscosity model to express the eddy viscosity term in the momentum equation (2) is motivated by:

- Recovering the proper behavior of the eddy viscosity near the wall in the case of the wall-bounded flows;
- Relying on the fact that no information about the direction and distance from the wall are needed (avoiding the use of any damping function);
- Being suitable for unstructured grids, where evaluating a distance to the wall is precarious.

The residual stress tensor of the WALE eddy viscosity model can be found as [3- 9]:

$$\nu_t = (C_w\Delta)^2 \frac{(s_{ij}^d s_{ij}^d)^{3/2}}{(\tilde{S}_{ij}\tilde{S}_{ij})^{5/2} + (s_{ij}^d s_{ij}^d)^{5/4}} \quad (8)$$

$$\text{Where: } s_{ij}^d = \frac{1}{2}(\tilde{g}_{ij}^2 + \tilde{g}_{ji}^2) - \frac{1}{3}\tilde{g}_{kk}^2\delta_{ij} \text{ And } \tilde{g}_{ij} = \frac{\partial \tilde{u}_i}{\partial x_j} \quad (9)$$

Cw: WALE model constant (*Cw* =0.49) [5-8]. And, Δ is the spatial filter width

B. Probability Density Function Approach

The statistical distribution function of the mixture fraction performs much better than the commonly used subgrid scale models perform for the mixture fraction variance [3-6, 10]. For non-premixed combustion, additional scalar variable of mixture fraction $\tilde{Z}(\vec{x},t)$ is needed. The transport equation of mixture fraction is such as [3,9],

$$\frac{\partial}{\partial t}\overline{\rho}\tilde{Z} + \frac{\partial}{\partial x_i}(\overline{\rho}u_i\tilde{Z}) = \frac{\partial}{\partial x_i}(\overline{\rho}D\frac{\partial}{\partial x_i}\tilde{Z}) \quad (10)$$

In the homogenous combustion the progress variable equation for non-premixed combustion [7-10],

$$\frac{\partial \overline{\rho}\tilde{c}}{\partial t} + \frac{\partial}{\partial x_i}(\overline{\rho}\tilde{u}_i\tilde{c}) = -\frac{\partial}{\partial x_i}\tau_c + \frac{\partial}{\partial x_i}.(\overline{\rho}D\frac{\partial}{\partial x_i}\tilde{c}) + \overline{\rho\dot{\omega}_c} \quad (11)$$

In this work, the probability density function (PDF) method is employed as a subgrid scale (SGS) closure in LES of a turbulent non-premixed combustion of Methane-Hydrogen/Air.

IV. Experimental Configuration and Application Domain

The configuration of the two coaxial jets confined within the combustor is given in figure 1. It was the focus of numerous investigations because of its relatively simple geometry and its similarity to power plant burner [3-5]. The cylindrical combustion chamber is of ray R_4=0.06115m and L=1m in length supplied by two coaxial jets, the central one has an internal ray R_1=0.03157 m and an external R_2=0.03175 m, which injects the methane with inlet mass flow rate and temperature respectively Q_1=0.0072 kg/s and T_1=300K. The annular one has an internal ray R_3= 0.04685m, that injects the air with an inlet mass flow rate Q_2=0.137 kg/s and preheated at a temperature T_2=750K. The combustion chamber is pressurized to 3.8atm and has a constant temperature wall of T_{wall}=500K [3-5].

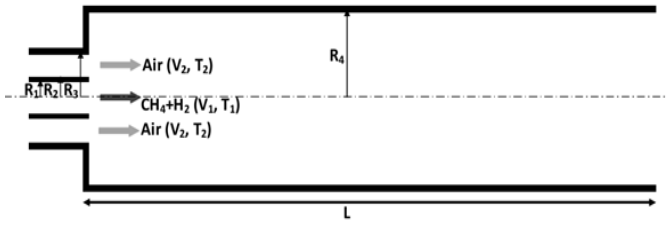

Fig. 1. Schematic of the burner.

V. Results and Discussion

We begin with the validation of the coupled models described previously with the experimental data [5]. After that, we introduce the effect of the hydrogen fuel injection with the methane. In addition, the same parameters used for the validation are used also to control the flame behavior supplied by the CH_4/H_2 mixture. Moreover, the presentation and comparison of results are based on normalizing length and velocity by using, respectively, the injector radius ($R \equiv R_3$) and the inlet bulk velocity of the air ($U \equiv V_2$).

A. Validation of Numerical Models

Figures 2 illustrate the comparison of the radial profiles of the average axial velocity obtained by the computational of coupled LES_WALE/PDF models and the experimental data [5]. In fact, the numerical results achieve significantly a good agreement with the experimental data. Thereby, the negative values of axial velocity in the x/R=0.14, 0.38 and 1.27 present the recirculating regions. Where, we observe the formation of two recirculating zones. The first one located in the center of the burner in the fuel jet level, generated by the delayed flow of the methane. And the second one caused by the brutal change in the burner section comparatively to the coaxial jets. However, the high values of velocity are located in the flame zone that is presented by the beak (x/R=1.27 and 4.67).

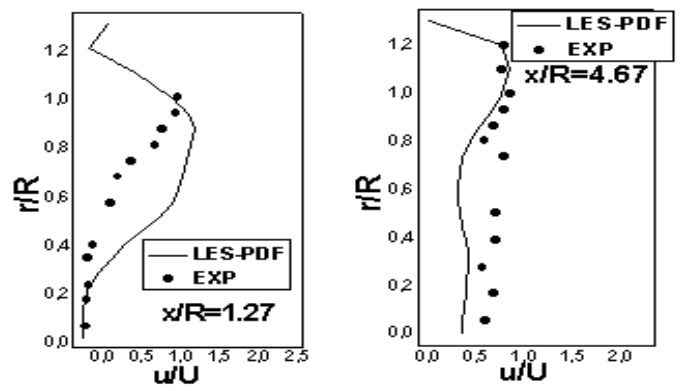

Fig. 2. Radial profiles of average axial velocity.

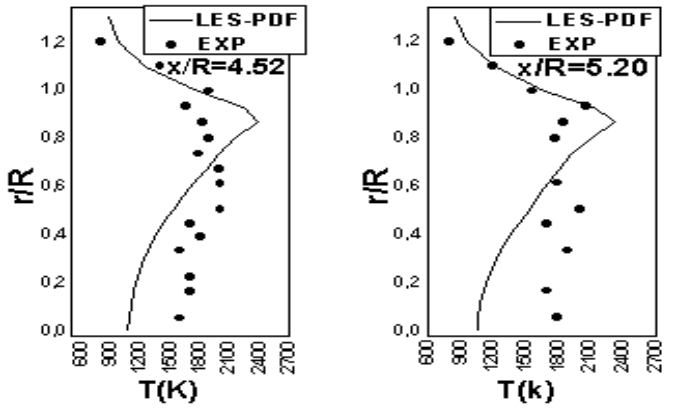

Fig. 3. Radial profiles of average temperature.

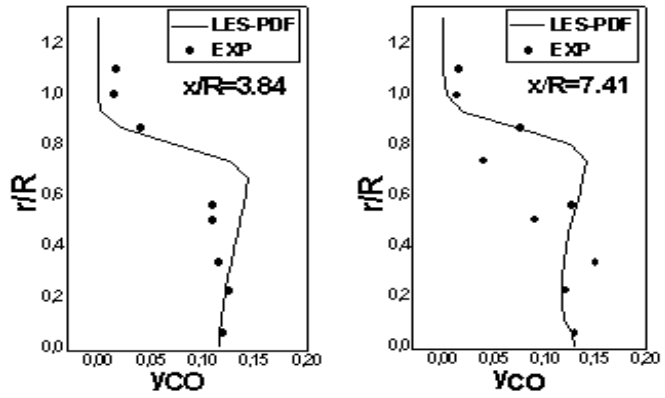

Fig. 4. Radial profiles of average Carbone monoxide mass fraction.

The comparisons of the predicted radial profiles of the average temperature with the experiments, [5], in different stations (x/R=4.52 and 5.20) in the burner is presented in figures 3; both numerical and experimental profiles have almost the same tendency. Whereas, the profiles characterized by the peak that presented the flame zone, where it seated on the shear layers that is the same zone where the fuel and the air are meeting. Whereas, the high temperature values are located around the flame region and the temperature begins decrease with the radial distance to achieve the wall temperature.

Figures 4 illustrate the comparison of predicted and experimental radial distribution of the carbon monoxide mass fraction for different stations in the burner for the stations x/R= 3.84 and 7.41. The computation predicted as well as the values of CO mass fraction comparatively to experimental data. Indeed, the height values of mass fraction of CO located in the center of the combustion chamber, which it decreases when going away from the center of the burner.

B. Impact of the Hydrogen Fuel Injection

The effect of hydrogen injection on the axial velocity in two stations (x/R=1.27 and 4.67) is illustrated in figures 5. These profiles are characterized by the peak in the two first stations, where in the last it disappears. The addition of the hydrogen on the reactive mixture gives a slight decrease in the axial velocity. In the first station, x/R=1.27, the profiles show the same tendency, where the production of the shearing zone presented by the peak situated approximately in the same position $0.35 \le \frac{r}{R} \le 1.2$. In x/R=4.67, the profiles are superimposed with a slight decrease in $0.3 \le \frac{r}{R} \le 0.75$ for reference case (CH_4=100%). And the case fuelled purely with hydrogen, H2=100%, illustrates the increase in the velocity ratio to exceed 1 ($\frac{u}{U} \ge 1$ for $0.5 \le \frac{r}{R} \le 1.2$). All cases are considered for the same inlet mass flow rate, but the inlet velocity is not same view the different density of each case. So, the slight mass of hydrogen relatively to methane results the increasing in the inlet velocity, where the hydrogen injection increases in the reactive mixture. Therefore, it influenced the flame velocity that has an impact on the burning products in the burner.

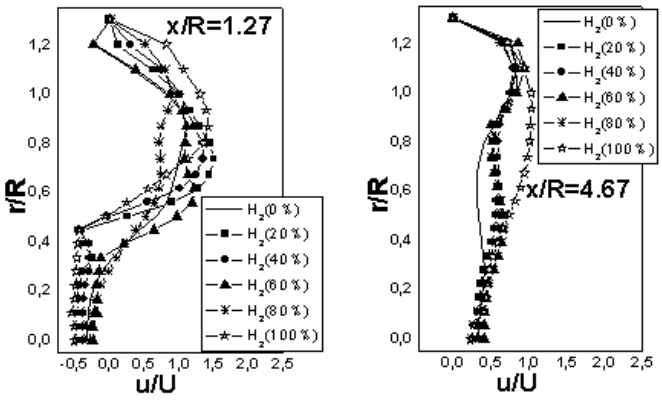

Fig. 5. Radial profiles of average axial velocity considered the hydrogen fuel injection

The behavior of temperature in the combustion chamber for different cases of the hydrogen injection is presented in the radial profiles of figures 6 for two stations, x/R=1.57 and 5.20. In the first station, x/R=0.89, the positions of peaks shifted to air jet level with the increase in maximum values of temperature for $H_2 \ge 80\%$. The temperature behavior in the center of combustion involves two depend cases of the

hydrogen quantity in the mixture ($H_2 \le 40$ for $T \approx 1100K$; $H_2 \ge 60$ for $T \approx 600K$). In the last station, x/R=5.20, the effect of the hydrogen enrichment decreases the temperature of 1200K for the reference case to achieve 600K for the flow supplied purely by H_2. Moreover, the profiles have the same positions and high values of the peaks. Thereafter, all computations in different hydrogen injection cases for the considered stations are present the shift in the peak according to the fuel composition, but they have slight difference in the maximum temperature.

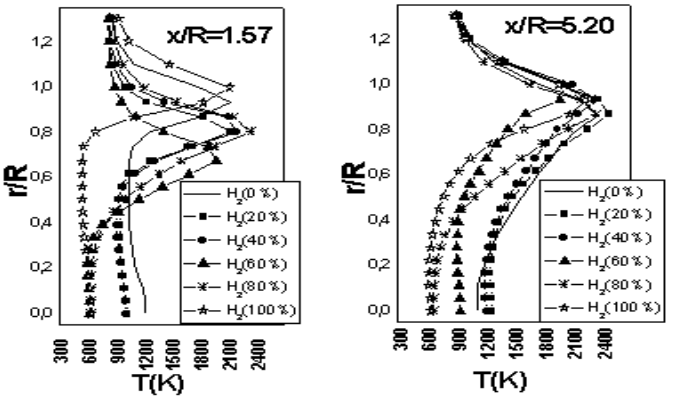

Fig. 6. Radial profiles of average temperature considered the hydrogen fuel injection.

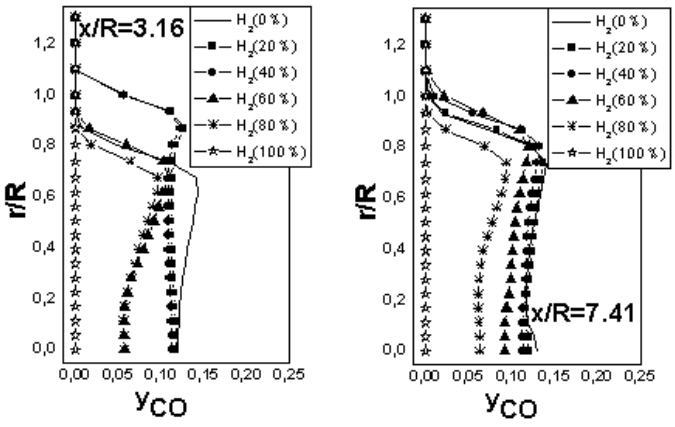

Fig. 7. Radial profiles of average Carbon monoxide considered the hydrogen fuel injection.

In order to control the chemical aspect of the methane enrichment by the hydrogen, we selected the carbon monoxide as a pollutant chemical species. We observed that carbon monoxide field various from and in between two stations in figures7, x/R=3.16 and 7.41, and all profiles decrease with radial distance. In the first station, x/R=0.21, the decrease of CO mass fraction with the increase H_2 to achieve the value 0 where $\frac{r}{R} \ge 0.75$. The profiles of second station, x/R=3.16, shows the same tendency with the first one; but the radial and longitudinal distribution are increasing by 100% relatively to the previous station. The last station, x/R=7.41, located far than the inlet of the burner but the production of CO is considerable and it's approximately the same to the previous station (x/R=3.16). Thereby, the effect of the hydrogen injection in the methane appears clearly under the reduction of CO when H_2 augmented. In addition, the carbon monoxide profiles show the same tendency with the temperature profiles. Therefore, in the centre of the combustion chamber the values of temperature and CO are elevated for the same percentage of the fuel composite (CH_4 and H_2); and they are decreasing when the hydrogen dominate the composition of the fuel.

VI. CONCLUSIONS

In this study, we recapitulate the validation of the coupled models LES/PDF and the effect of the hydrogen enrichment on the methane flame, considering the different compositions of the hydrogen and the methane in the inlet fuel supplied the combustor, using the FLUENT-CFD package to carry out the computations. The conclusions arising from this investigation are as follow:

- The computational results of the coupled dynamic model, LES, and scalar model, PDF, give a satisfactory agreement with the experiment data;
- The important role of the shear layers caused by velocity ratio between the fuel and the air to establish the flame in the burner;
- The rich region is located on the shear layers where the flame is seated;
- The relation between the temperature and the carbon monoxide is proportional. That is the temperature decrease when the hydrogen increase in the reactive mixture,
- The H_2 augmentation in the fuel mixture improves flame velocity;
- The addition of the H_2 in the reactive mixture reduces the emission of CO in the combustion produced species.

REFERENCES

[1] E. Hu, Z. Huang, J. Zheng, Q. Li, J. He, "Numerical study on laminar burning velocity and NO formation of premixed methane–hydrogen–air flames," International journal of hydrogen energy, vol.34, pp.6545–6557, 2009.

[2] F.Tabet, B.Sarhb, I.Gokalp, "Hydrogen–hydrocarbon turbulent non-premixed flame structure," International journal of hydrogen energy, vol.34, pp.5040–5047, 2009.

[3] F. Bouras, A.Soudani, and M. Si Ameur, "Thermochemistry Study of Internal Combustion Engine," Energy Procedia, vol.18, pp.1086–1095, 2012.

[4] F.Bouras, M.E.Attia and F.Khaldi, "Improvements of the Combustion Characteristics by the Hydrogen Enrichment,"CEIT 2015 Conference Publications, http://ieeexplore.ieee.org/xpl/articleDetails.jsp?arnumber=7233003.

[5] C.P. Pierce, P. Moin, "Progress-Variable Approach for Large-Eddy Simulation of Non-Premixed Turbulent Combustion," Journal of Fluid Mechanics, vol. 504, pp 73–97, 2004.

[6] F. Bouras, A. Soudani, and M. Si Ameur, "Large Eddy Simulation for Lean Premixed Combustion," Canadian Journal of Chemical Engineering, vol.91, pp.231–237, 2013.

[7] F. Bouras, A. Soudani, and M. Si Ameur, "Numerical Study of the Turbulent Flow Inside an ORACLES Configuration," Trans.ASME, Journal of Appllied Mechnics, vol. 79, 51014, 2012.

[8] F. Bouras, "Numerical study of turbulent structures for lean premixed prevaporized combustion," Journal of Applied Mechanics and Technical Physics, vol. 55, pp.614–626, 2014.

[9] F. Bouras, F. Khaldi," Computational Modeling of Thermodynamic Irreversibilities in Turbulent Non-Premixed Combustion," Heat and Mass Transfer, vol.52, pp. 671–681, 2016.

[10] H. Wang, Y. Chen, "PDF modelling of turbulent non-premixed combustion With detailed chemistry," Chemical Engineering Science, vol.59, pp. 3477–3490, 2004.